Article

Kinetic and Thermodynamic Analysis of the Hydrolytic Ring-Opening of the Malondialdehyde–Deoxyguanosine Adduct, 3-(2‘-Deoxy-β-d-*erythro*-pentofuranosyl)- pyrimido[1,2-]purin-10(3*H*)-one

James N. Riggins, J. Scott Daniels, Carol A. Rouzer, and Lawrence J. Marnett

J. Am. Chem. Soc., **2004**, 126 (26), 8237-8243• DOI: 10.1021/ja040009r • Publication Date (Web): 09 June 2004

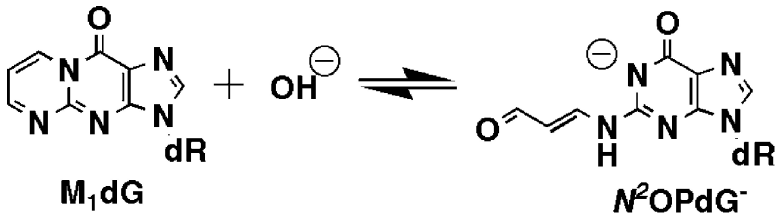

M_1dG N^2OPdG^-

J|A|C|S
ARTICLES
Published on Web 06/09/2004

Kinetic and Thermodynamic Analysis of the Hydrolytic Ring-Opening of the Malondialdehyde−Deoxyguanosine Adduct, 3-(2′-Deoxy-β-D-*erythro*-pentofuranosyl)-pyrimido[1,2-α]purin-10(3*H*)-one

James N. Riggins, J. Scott Daniels, Carol A. Rouzer, and Lawrence J. Marnett*

Contribution from the A. B. Hancock Jr. Memorial Laboratory for Cancer Research, Departments of Biochemistry and Chemistry, Vanderbilt Institute of Chemical Biology, Center in Molecular Toxicology, Vanderbilt-Ingram Cancer Center, Vanderbilt University School of Medicine, Nashville, Tennessee 37232-0146

Received January 7, 2004; E-mail: larry.marnett@vanderbilt.edu

Abstract: 3-(2′-Deoxy-β-D-*erythro*-pentofuranosyl)pyrimido[1,2-α]purin-10(3*H*)-one (M_1dG) is the major reaction product of deoxyguanosine with malondialdehyde or base propenals. M_1dG undergoes hydrolytic ring-opening to N^2-oxopropenyl-deoxyguanosine (N^2OPdG) under basic conditions. We report that ring-opening of M_1dG as a nucleoside or in oligonucleotides is a reversible second-order reaction with hydroxide ion. NMR and UV analysis revealed N^2OPdG$^-$ to be the only product of M_1dG ring-opening in basic solution. The rate constant for reaction of M_1dG with hydroxide is 3.8 M^{-1} s^{-1}, and the equilibrium constant is calculated to be $2.1 \pm 0.3 \times 10^4$ M^{-1} at 25 °C. Equilibrium constants determined by spectroscopic analysis of the reaction end-point or by thermodynamic analysis of rate constants determined over a range of temperatures yielded a value $2.5 \pm 0.2 \times 10^4$ M^{-1}. Kinetic analysis of ring-opening of M_1dG in oligonucleotides indicated the rate constant for ring-opening is decreased 10-fold compared to that in the nucleoside. Flanking purines or pyrimidines did not significantly alter the rate constants for ring-opening, but purines flanking M_1dG enhanced the rate constant for the reverse reaction. A mechanism is proposed for ring-opening of M_1dG under basic conditions and a role is proposed for duplex DNA in accelerating the rate of ring-opening of M_1dG at neutral pH.

Introduction

DNA damage is an important step in the induction of genetic mutations by foreign chemicals or endogenously generated electrophiles or free radicals.[1−5] Malondialdehyde (β-hydroxyacrolein), a bifunctional electrophile generated from polyunsaturated fatty acids as a result of oxidative stress, reacts with DNA bases to form adducts to dG, dA, and dC.[6] The most abundant adduct is to dG: 3-(2′-deoxy-β-D-*erythro*-pentofuranosyl)pyrimido[1,2-α]purin-10(3*H*)-one. This adduct has been termed M_1dG to distinguish it from other dG adducts formed in low yields from oligomers of malondialdehyde. M_1dG is a strong block to DNA replication and is mutagenic in bacteria and mammalian cells.[7,8] A number of reports indicate that M_1dG is present in genomic DNA of healthy human beings,[9−15] and M_1dG has recently been reported to be present in human urine.[16]

Recent reports from our laboratory reveal that M_1dG is electrophilic and reacts with a variety of nucleophiles including hydroxide, amines, hydroxylamines, and hydrazines.[17−20] M_1dG is the first DNA adduct to be demonstrated to constitute a reactive intermediate *within* duplex DNA.[21,22] Similar chemistry has subsequently been described for other exocyclic adducts

(1) Bartsch, H. *Mutat. Res.* **1996**, *340*, 67−79.
(2) Gupta, R. C.; Lutz, W. K. *Mutat. Res.* **1999**, *424*, 1−8.
(3) Hecht, S. S. *Chem. Res. Toxicol.* **1998**, *11*, 559−603.
(4) Farmer, P. B.; Shuker, D. E. *Mutat. Res.* **1999**, *424*, 275−286.
(5) Marnett, L. J.; Plastaras, J. P. *Trends Genet.* **2001**, *17*, 214−221.
(6) Marnett, L. J. *IARC Sci. Publ.* **1999**, 17−27.
(7) Fink, S. P.; Reddy, G. R.; Marnett, L. J. *Proc. Natl. Acad. Sci. U. S. A.* **1997**, *94*, 8652−8657.
(8) Seto, H.; Seto, T.; Takesue, T.; Ikemura, T. *Chem. Pharm. Bull. (Tokyo)* **1986**, *34*, 5079−5085.
(9) Everett, S. M.; Singh, R.; Leuratti, C.; White, K. L.; Neville, P.; Greenwood, D.; Marnett, L. J.; Schorah, C. J.; Forman, D.; Shuker, D.; Axon, A. T. *Cancer Epidemiol. Biomarkers Prev.* **2001**, *10*, 369−376.
(10) Leuratti, C.; Singh, R.; Lagneau, C.; Farmer, P. B.; Plastaras, J. P.; Marnett, L. J.; Shuker, D. E. *Carcinogenesis* **1998**, *19*, 1919−1924.
(11) Leuratti, C.; Singh, R.; Deag, E. J.; Griech, E.; Hughes, R.; Bingham, S. A.; Plastaras, J. P.; Marnett, L. J.; Shuker, D. E. *IARC Sci. Publ.* **1999**, 197−203.
(12) Leuratti, C.; Watson, M. A.; Deag, E. J.; Welch, A.; Singh, R.; Gottschalg, E.; Marnett, L. J.; Atkin, W.; Day, N. E.; Shuker, D. E.; Bingham, S. A. *Cancer Epidemiol. Biomarkers Prev.* **2002**, *11*, 267−273.
(13) Singh, R.; Leuratti, C.; Josyula, S.; Sipowicz, M. A.; Diwan, B. A.; Kasprzak, K. S.; Schut, H. A.; Marnett, L. J.; Anderson, L. M.; Shuker, D. E. *Carcinogenesis* **2001**, *22*, 1281−1287.
(14) Chaudhary, A. K.; Nokubo, M.; Reddy, G. R.; Yeola, S. N.; Morrow, J. D.; Blair, I. A.; Marnett, L. J. *Science* **1994**, *265*, 1580−1582.
(15) Rouzer, C. A.; Chaudhary, A. K.; Nokubo, M.; Ferguson, D. M.; Reddy, G. R.; Blair, I. A.; Marnett, L. J. *Chem. Res. Toxicol.* **1997**, *10*, 181−188.
(16) Hoberg, A.; Otteneder, M.; Marnett, L. J.; Poulsen, H. E. *J. Mass Spectrom.* **2003**. In press.
(17) Niedernhofer, L. J.; Riley, M.; Schnetz-Boutaud, N.; Sanduwaran, G.; Chaudhary, A. K.; Reddy, G. R.; Marnett, L. J. *Chem. Res. Toxicol.* **1997**, *10*, 556−561.
(18) Schnetz-Boutaud, N.; Daniels, J. S.; Hashim, M. F.; Scholl, P.; Burrus, T.; Marnett, L. J. *Chem. Res. Toxicol.* **2000**, *13*, 967−970.
(19) Otteneder, M.; Plastaras, J. P.; Marnett, L. J. *Chem. Res. Toxicol.* **2002**, *15*, 312−318.
(20) Otteneder, M.; Scott Daniels, J.; Voehler, M.; Marnett, L. J. *Anal. Biochem.* **2003**, *315*, 147−151.
(21) Mao, H.; Reddy, G. R.; Marnett, L. J.; Stone, M. P. *Biochemistry* **1999**, *38*, 13491−13501.

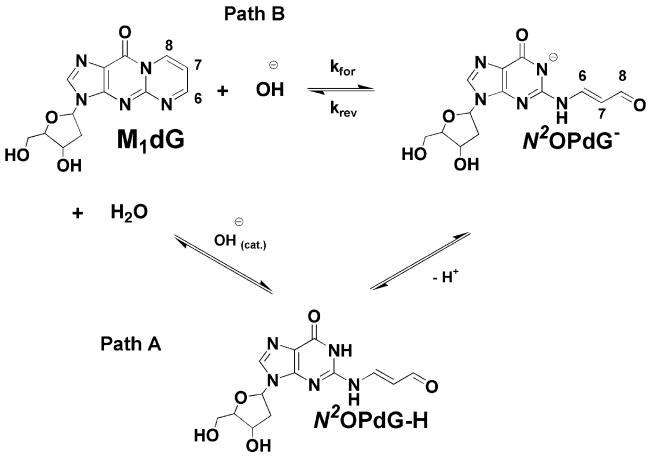

Figure 1. Reaction of M_1dG with OH^- to yield N^2OPdG^-.

derived from bifunctional electrophiles.[23,24] Of particular interest are several reports demonstrating that M_1dG and other exocyclic adducts undergo quantitative ring-opening when introduced into duplex DNA opposite dC residues. For example, M_1dG hydrolytically ring-opens to N^2-oxopropenyl-deoxyguanosine (N^2OPdG) when placed opposite dC but not when placed opposite dT. In vivo mutagenesis experiments in which singly adducted viral genomes containing M_1dG opposite dC or dT are replicated in bacteria indicate that the ring-closed form of the adduct is substantially more mutagenic than the ring-opened form.[7,25]

The kinetics and mechanism of the hydrolytic ring-opening of M_1dG either as the nucleoside or in single- or double-stranded nucleic acids have not been reported. A preliminary report from our laboratory demonstrated that the nucleoside M_1dG undergoes hydrolysis to N^2OPdG at basic pH.[26] We proposed that hydroxide catalyzes water addition (Figure 1, path A) and shifts the equilibrium toward product by deprotonation of the imino proton of N^2OPdG (assumed to have a pK_a comparable to that of dG). In the present contribution, we report the results of a detailed study of the kinetics of M_1dG hydrolysis at basic pH. The results indicate that hydroxide does not catalyze hydrolysis but is a reactant that adds directly to M_1dG to form the N^2OPdG anion (N^2OPdG^-). Hydroxide addition at elevated pH is reversible such that an equilibrium exists between M_1dG and N^2OPdG^- (Figure 1, path B). K_{eq} was evaluated independently by kinetic, spectroscopic, and thermodynamic methods. In addition, experiments in single-stranded DNA evaluated the rates of ring-opening and ring-closing as a function of sequence context. These experiments enable us to propose a mechanism for ring-opening of M_1dG in duplex DNA.

Results

Ring-Opening of M_1dG. To analyze the conversion of M_1dG to N^2OPdG^-, differences in UV absorption and fluorescence emission spectra were exploited. Both adducts exhibit absorbance bands between 300 and 380 nm but with different absorptivities (M_1dG -λ_{max} = 320; ϵ= 5,100, λ_{max} = 350; ϵ= 3,300 $M^{-1}cm^{-1}$; N^2OPdG^- -λ_{max} = 320; ϵ= 28,800 $M^{-1}cm^{-1}$). M_1dG is fluorescent upon excitation at 363 nm (λ_{emit}= 511 nm) and has a quantum yield of 0.12 (measured by comparison against quinine sulfate standard) whereas, N^2OPdG^- is not fluorescent under these excitation conditions (Figure 2). The conversion of M_1dG to N^2OPdG^- in basic, aqueous solution

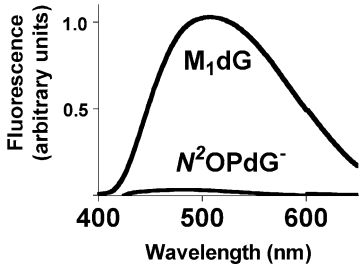

Figure 2. Fluorescence properties of M_1dG and N^2OPdG^-. Overlayed fluorescence emission spectra are shown for the adduct in 0.25 M sodium phosphate buffer at pH 6.5 (M_1dG) and 11.0 (N^2OPdG^-) upon excitation at 363 nm.

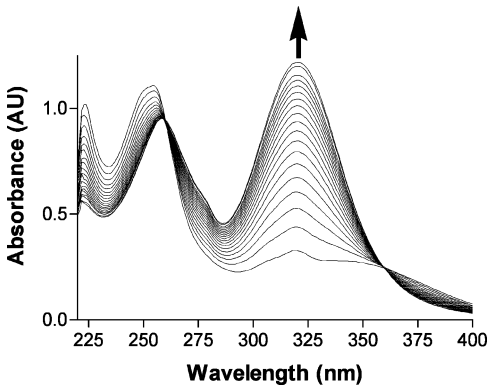

Figure 3. UV absorption spectra for base-treated M_1dG at various times. 5.0×10^{-5} M M_1dG was ring-opened using 0.25 M sodium phosphate buffer at pH 11.2 at 25 °C. The absorbance increase over time at 320 nm is illustrated by the arrow. Spectra were accumulated at 20-s intervals. Isosbestic points are observed at 363 nm and at 258 nm.

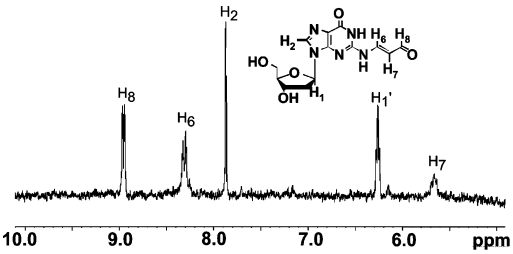

Figure 4. ^1H NMR spectrum of N^2OPdG^- in D_2O. M_1dG (0.001 g) was dissolved in 1 mL of 0.25 M sodium phosphate buffer (pH 11.2), dried, and dissolved in 1 mL of D_2O.

(0.25 M sodium phosphate, pH 11.0) followed by UV spectroscopy is displayed in Figure 3. An increase in the absorbance at 320 nm is seen over time, consistent with the formation of N^2OPdG^-. Isosbestic points attributed to the adduct are observed at 363 nm and at 258 nm. The observation of two isosbestic points implies the conversion of M_1dG to N^2OPdG^- is the only reaction occurring. Figure 4 displays the ^1H NMR spectrum for base-treated M_1dG, confirming the solution contains only N^2OPdG^-.[26] The resonances and coupling constants for protons 6, 7 and 8 (8.3 ppm, J = 13 Hz; 5.6 ppm, J = 9, 13 Hz; and 9.0 ppm, J = 9 Hz, respectively) indicate that N^2OPdG^- is in the trans orientation about the 6,7-double bond.

(22) Mao, H.; Schnetz-Boutaud, N. C.; Weisenseel, J. P.; Marnett, L. J.; Stone, M. P. *Proc. Natl. Acad. Sci. U.S.A.* **1999**, *96*, 6615−6620.
(23) Sanchez, A. M.; Minko, I. G.; Kurtz, A. J.; Kanuri, M.; Moriya, M.; Lloyd, R. S. *Chem. Res. Toxicol.* **2003**, *16*, 1019−1028.
(24) de los Santos, C.; Zaliznyak, T.; Johnson, F. *J. Biol. Chem.* **2001**, *276*, 9077−9082.
(25) Fink, S. P.; Marnett, L. J. *Mutat. Res.* **2001**, *485*, 209−218.
(26) Reddy, G. R.; Marnett, L. J. *J. Am. Chem. Soc.* **1995**, *117*, 5007−5008.

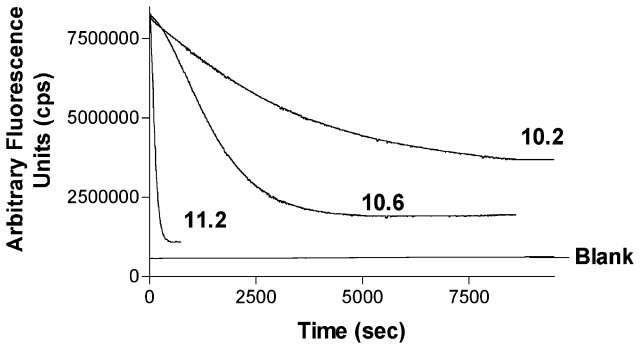

Figure 5. Sample kinetic decay plots for M_1dG fluorescence. M_1dG (10 μM) was ring-opened in 0.25 M sodium phosphate buffers at various pHs at 25 °C. Fluorescence was monitored over time at 511 nm (ex 363 nm). Data were accumulated until the overall fluorescence was no longer changing. Blank runs were made with 0.25 M sodium phosphate, pH 11.0. Similar decay plots were monitored at different temperatures for thermodynamic analysis (data not shown).

Table 1. Values of k_{obs} for M_1dG Ring-Opening

	$k_{obs} \times 10^{-4}$ (s^{-1})				
[OH-] (10^{-6} M)	25 °C	35 °C	45 °C	55 °C	60 °C
1000	36.3	95.6	225	283	437
561	30.5	79.7	158	198	291
251	11.2	31.4	87.5	110	154
100	3.9	8.7	36.6	53.6	98.3
32	1.4	6.7	16.4	21.6	67.6

To evaluate the kinetics of hydrolytic ring-opening, absorbance increases and fluorescence decays were monitored under basic conditions. Pseudo-first-order conditions with respect to hydroxide were maintained for a given sample by using phosphate buffers. Changes in absorbance or fluorescence were followed until the reaction reached a plateau. Representative fluorescence decay plots are displayed in Figure 5 and reveal an exponential decrease in M_1dG concentration, indicating the reaction is first-order with respect to M_1dG. The existence of a plateau at each pH indicates that an equilibrium is being reached and that the position of the equilibrium is dependent upon the concentration of hydroxide. This suggests that ring-opening involves the addition of hydroxide to M_1dG rather than hydroxide acting as a catalyst. Similar observations were made by monitoring absorbance increases upon ring-opening. The fluorescence decay observable upon treating M_1dG with base was fit to a single-exponential decrease function. Decay plots were followed for a range of hydroxide concentrations and yielded values for the observed first-order rate constants (k_{obs}). These data are compiled in Table 1.

A plot of k_{obs} versus hydroxide is linear and regression analysis reveals a nonzero *y*-intercept (Figure 6). This observation suggests a model where the reaction is first-order with respect to hydroxide and is reversible. The data fit the equation:

$$k_{obs} = k_{for}[OH^-] + k_{rev} \quad (1)$$

The slope of the plot in Figure 6 yields k_{for}, and the *y*-intercept provides k_{rev}.

Rate data for the ring-opening reaction were obtained over a temperature range from 25 to 60 °C (Figure 6) and a pH range of 8.6−12. Determinations were not made at pH values above 12 because the reaction is too fast to observe reliably at high pH. Also, at pH values above 12, hydrolysis of N^2OPdG$^-$ to

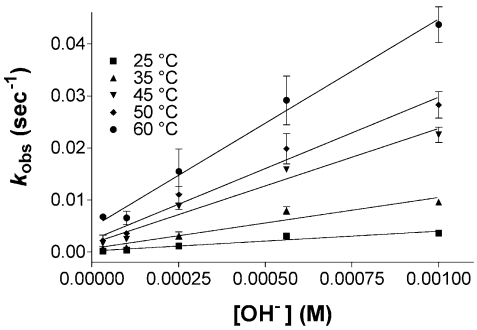

Figure 6. Plot of k_{obs} vs [OH$^-$]. k_{obs} values measured at the indicated temperatures were obtained by one-phase exponential curve fitting of fluorescence decay plots using Prism software. All data points shown reflect triplicate measurements. Error is shown for each point. For some points, the error was masked in the point itself and is not observable.

Table 2. Kinetic and Thermodynamic Values for M_1dG and M_1dG-5′-phosphate Ring-Opening[a]

parameter	M_1dG	M_1dG-5′-phosphate
$k_{forward}$[b] (M^{-1} s^{-1})	3.8 ± 0.06	2.3 ± 0.1
$k_{reverse}$[b] (s^{-1})	$1.8 \times 10^{-4} \pm 0.3$	1.4×10^{-4}
K_{eq} from k_{for}/k_{rev} (M^{-1})	$2.11 \pm 0.25 \times 10^4$	$1.63 \pm 0.50 \times 10^4$
K_{eq} from $\Delta G°$ (M^{-1})	2.51×10^4	2.01×10^4
K_{eq}[c] plateau (M^{-1})	$2.51 \pm 0.25 \times 10^4$	N/A
E_a forward (kJ mol^{-1})	56.2 ± 5.5	72.0 ± 4.7
E_a reverse (kJ mol^{-1})	78.2 ± 3.8	117.6 ± 8.8
$\Delta H°$ (kJ mol^{-1})	-21.9 ± 1.8	-43.5 ± 3.9
$\Delta S°$ (kJ mol^{-1} K^{-1})	$+0.010 \pm 0.005$	-0.065 ± 0.012
$\Delta G°$ (kJ mol^{-1})	-24.8 ± 3.3	-24.0 ± 0.3

[a] Loss of M_1dG or M_1dG-5′-phosphate due to treatment with buffers at basic pH was monitored by a decrease in fluorescence. Kinetic values were determined by fitting fluorescence decay plots to one-phase exponential functions. Determinations of $k_{forward}$ and $k_{reverse}$ were made at 25, 35, 45, 55, and 60 °C. Thermodynamic values were determined through Arrhenius and van't Hoff plots. [b] Values reported in table were determined at 25 °C (298 K). [c] K_{eq} was determined from the ratio of [N^2OPdG$^-$]/[M_1dG] at the equilibrium point of the reaction.

2′-deoxyguanosine and the enolate of malondialdehyde becomes significant (Supporting Information, 2). K_{eq} was determined from the quotient of k_{for} and k_{rev} (Table 2). The value of K_{eq} at 25 °C was calculated from these data to be $2.1 \pm 0.2 \times 10^4$ M^{-1} and corresponds to a $\Delta G°$ of -24.6 kJ mol^{-1}.

The K_{eq} at 25 °C was also obtained by determining the relative concentrations of M_1dG and N^2OPdG$^-$ in solution at varying pHs. Samples of M_1dG were allowed to equilibrate, and the concentrations of M_1dG and N^2OPdG$^-$ were determined by fluorescence spectroscopy. The ratio of N^2OPdG$^-$ and M_1dG is equal to the product of the equilibrium constant and the concentration of hydroxide.

$$\frac{[N^2\text{OPdG}^-]}{[\text{M}_1\text{dG}]} = K_{eq}[OH^-] \quad (2)$$

The ratio of adduct concentrations was then plotted as a function of the hydroxide concentration. Figure 7 shows the plot observed

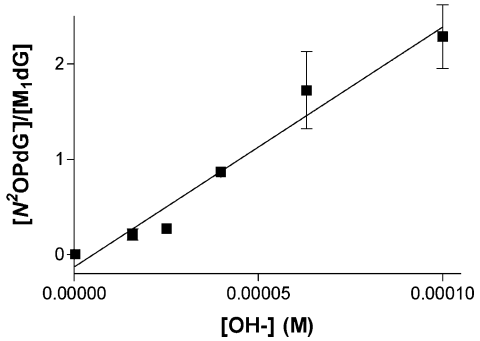

Figure 7. Determination of K_{eq} by end-point analysis. M_1dG was incubated in 0.25 M sodium phosphate buffers at various pHs for 3 h at 25 °C. Triplicate samples were measured. The fluorescence for each sample was determined and used to calculate the ratio of M_1dG to N^2OPdG$^-$. A sample at pH 11.5 was used as a marker for 100% N^2OPdG$^-$. Error is shown for all points. For some points, the error was masked in the point itself and is not observable.

using fluorescence emission as an indicator of M_1dG remaining in solution and yields a slope of $2.5 \pm 0.3 \times 10^4$ M^{-1}. $\Delta G°$ calculated from this value for K_{eq} is -25.1 kJ mol^{-1} (Table 2).

The kinetic experiments, completed over a range of temperatures, allows for an analysis of the thermodynamics of the ring-opening. Only a 35 °C range was evaluated due to anticipated adduct instability at elevated temperature. Activation energy (E_a) was determined from Arrhenius plots for the forward and reverse reactions (Figure 8, panels A and B, respectively), and equilibrium constants were analyzed in a similar manner using a van't Hoff plot (Figure 9) to obtain values for $\Delta H°$ and $\Delta S°$ (Table 2). Ring-opening was found to be exothermic ($\Delta H° = -21.9 \pm 1.8$ kJ mol^{-1}) and resulted in a small change in the entropy of the system ($\Delta S° = 0.010 \pm 0.005$ kJ mol^{-1} K^{-1}). $\Delta G°$ was calculated from these extrapolated values to be -24.8 ± 3.3 kJ mol^{-1}, which corresponds to a K_{eq} of 2.5×10^4 M^{-1}.

The error in the determination of K_{eq} was calculated for the three different methods used. The error in K_{eq} derived from the ratio of k_{for} and k_{rev} was approximately 12%. This arises primarily from the extrapolation of k_{rev} in the linear plot above, which yields a value of $1.8 \pm 0.3 \times 10^{-4}$ s^{-1}. Comparable error (10%) was measured when the ratio of adduct concentrations at equilibrium were used to determine K_{eq}. This is most likely due to limits in sensitivity in the fluorescence and the reliability of the spectrofluorometer to measure small differences in the fluorescence of samples at nearly 100% N^2OPdG$^-$. Error in $\Delta G°$ for the thermodynamic analysis was 13%, and affected the accuracy of the K_{eq} determined from this treatment of the data. Extrapolation of $\Delta S°$ in the van't Hoff analysis gave greater error in $\Delta G°$. While the error found in these experiments was consistently 10−13%, the fact that similar values for K_{eq} could be calculated from the different methods lends support to the validity of the results observed in the kinetic and thermodynamic studies.

Ring-Opening of M_1dG in Oligonucleotides. Having determined kinetic and thermodynamic parameters for the ring-opening reaction in the monomer, the same experimental analysis for ring-opening in oligonucleotides bearing M_1dG was conducted. Four 8-mer oligonucleotide sequences with M_1dG placed at position 4 were synthesized. Oligonucleotide sequences containing the adduct were chosen on the basis of differences in flanking sequence to determine any possible effects that neighboring bases may have on the reaction. Oligonucleotide

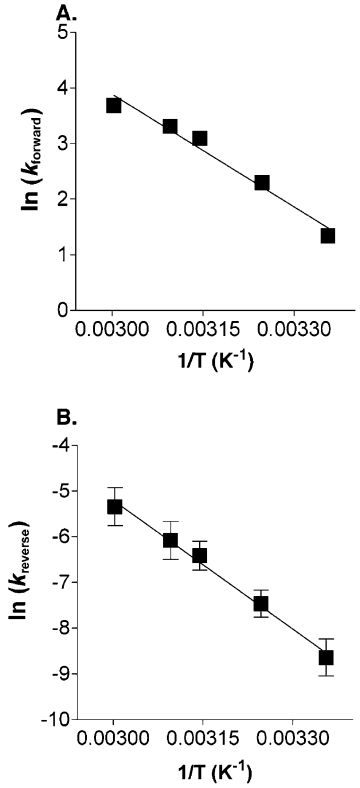

Figure 8. Arrhenius plots for the forward and reverse rate constants obtained from the data in Figure 3. From these plots the activation energy (E_a) and frequency factor (A) for the forward and reverse reactions were determined using linear regression analysis. Error in this analysis was propagated for the fitted data using the relationship:[31] $\delta \ln(k_{for}) = \delta k_{for}/k_{rev}$ or $\delta \ln(k_{rev}) = \delta k_{rev}/k_{rev}$. Error for the Arrhenius plot of the forward rate constants was small enough to be contained within the points displayed.

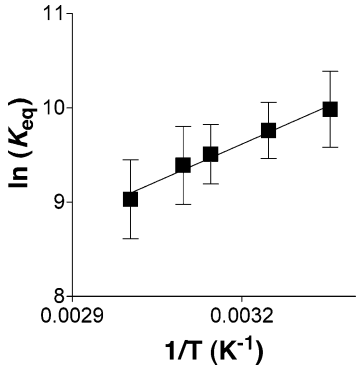

Figure 9. van't Hoff analysis of the equilibrium constants determined from the forward and reverse rate constants observed from Figure 6. ΔH and ΔS values were obtained from this plot. Error in the quotient of k_{for} and k_{rev} was propagated using the following function:[31] $\delta(K_{eq}) = (K_{eq})[(\delta k_{for}/k_{rev})^2 + (\delta k_{rev}/k_{rev})^2]^{1/2}$ followed by $\delta \ln(K_{eq}) = \delta K_{eq}/K_{eq}$.

fluorescence was measured over time after treatment with phosphate buffers at different pHs. Plots of the change in fluorescence over time were fit to a single exponential to obtain k_{obs} values (see Supporting Information for values), and then k_{for} and k_{rev} were extracted from the fitted data as described above for the monomer (Table 3). Experiments at varying temperature followed by Arrhenius and van't Hoff analysis gave thermodynamic parameters for the ring-opening reaction in oligonucleotides. The results, which are an average of at least three data sets, are summarized in Table 3.

Table 3. Kinetic and Thermodynamic Values for M_1dG Oligonucleotide Ring-Opening[a]

parameter	AXA8mer[c]	CXC8mer[c]	GXG8mer[c]	TXT8mer[c]
$k_{forward}$ (M^{-1} s^{-1})[b]	0.32 ± 0.05	0.36 ± 0.07	0.37 ± 0.04	0.42 ± 0.06
$k_{reverse}$ (10^{-4} s^{-1})[b]	3.8 ± 0.5	1.7 ± 0.7	5.6 ± 0.4	1.0 ± 0.7
K_{eq} (10^3 M^{-1})	0.8 ± 0.2	2.2 ± 0.4	0.7 ± 0.1	4.2 ± 0.8
E_a forward (kJ/mol)	55 ± 7	52 ± 3	41 ± 1	36 ± 5
E_a reverse (kJ/mol)	78 ± 6	92 ± 5	110 ± 9	76 ± 8
$\Delta H°$ (kJ/mol)	−15 ± 3	−40 ± 7	−70 ± 8	−41 ± 5
$\Delta S°$ (kJ/molK)	−0.011 ± 0.009	−0.053 ± 0.02	−0.18 ± 0.02	−0.067 ± 0.016
$\Delta G°$ (kJ/mol)	−17.0 ± 0.2	−23.0 ± 0.5	−16 ± 2	−21.0 ± 0.4

[a] Loss of M_1dG in adducted oligonucleotides due to treatment with buffers at basic pH was monitored as a decrease in fluorescence. Determinations of $k_{forward}$ and $k_{reverse}$ were done at 25, 35, 45, 55, and 60 °C. Kinetic values were determined by fitting fluorescence decay plots to one-phase exponential functions. Thermodynamic values were determined through Arrhenius and van't Hoff plots. [b] Values reported in table are for 25 °C. [c] Full sequence is 5′-GGYXYCCG-3′ where X = M_1dG and Y = A, C, G, or T.

In all cases, the rate constants for ring-opening of the adduct were reduced approximately 10-fold (0.32−0.42 M^{-1} s^{-1}) in the oligonucleotides when compared to k_{for} for M_1dG. However, no large sequence-dependent changes in k_{for} were observed in the four oligonucleotides tested. On the other hand, reverse rate constants for the adduct in the oligonucleotides were found to be on the same order of magnitude as that observed in the monomer and were found to be dependent upon the sequence context. The reverse rate constants for oligonucleotides differed by up to 6-fold among the sequences tested, accounting for the differences in the calculated K_{eq} values (Table 3). K_{eq} values under these conditions, for all oligonucleotides tested, were smaller than those for the reaction of M_1dG. The K_{eq} values measured for the sequences containing flanking pyrimidines were higher than those observed for sequences with flanking purines.

Thermodynamics for ring-opening in oligonucleotides also showed some striking sequence dependencies (Table 3). When pyrimidines flanked the adduct site, ring-opening was found to be exothermic; the absolute value of the enthalpy change was doubled when compared to the value for the nucleoside. The change in the entropy of the reaction became negative for these oligonucleotides. $\Delta G°$ was negative and was dominated by the change in the enthalpy of the solution. The contribution of entropy to the $\Delta G°$ of the reaction, in contrast to that observed in the nucleoside, was substantial. Values for $\Delta H°$, $\Delta S°$, and $\Delta G°$ obtained for the 5′-C-X-C-3′ and 5′-T-X-T-3′ sequences were nearly equivalent. The thermodynamics observed for ring-opening in purine flanking sequences were more complex. While in both purine flanking sequences the enthalpy and entropy were negative, the absolute value of the enthalpy change in the 5′-G-X-G-3′ sequence was approximately 4.5 times that observed for the 5′-A-X-A-3′ oligonucleotide. Overall, the $\Delta G°$ for the two purine flanking sequences was the same and reveals that the equilibrium was more disfavored in these sequences than in the pyrimidine flanking sequences.

One possible explanation for the observed differences in ring-opening between the nucleoside and oligonucleotides is the involvement of negative charge in oligonucleotides and its effect on the susceptibility of the adduct to reaction. To attempt to address this issue, similar kinetic and thermodynamic experiments were performed with the 5′-phosphate of M_1dG, and the results are compiled in Table 2. A small but significant reduction in the forward rate constant of ring-opening for the nucleotide was observed when compared with rate constants determined for the adduct nucleoside. The nucleotide thermodynamics behave in a manner similar to those observed for oligonucleotides. The absolute value of the enthalpy change for ring-opening is doubled with respect to that for the nucleoside, and the entropy for the reaction became negative. The $\Delta G°$ for the reaction of the nucleotide was only slightly reduced when compared to that of the nucleoside.

Table 4. Ratio of N^2OPdG$^-$ to M_1dG at Various pHs

pH/[OH^-]	M_1dG	AXA8mer	TXT8mer
11 (1 mM)	21.5	0.84	4.2
9 (0.01 mM)	0.215	0.00084	0.0042
7 (0.0001 mM)	0.000215	0.0000084	0.000042
K_{eq}[a] (10^3 M^{-1})	**21.5**	**0.8**	**4.2**

[a] K_{eq} here is determined from the quotient of k_{for} and k_{rev} calculated in the kinetic assays.

Discussion

In this study, the kinetics and thermodynamics of M_1dG conversion to N^2OPdG$^-$ under basic conditions were evaluated. The data for ring-opening show that the bimolecular rate constant for ring-opening is 3.8 M^{-1} s^{-1} at 25 °C. The reverse rate constant is much smaller (1.8×10^{-4} s^{-1}), giving an equilibrium constant of $2.1 \pm 0.3 \times 10^4$ M^{-1}. Under standard conditions, the free energy change for ring-opening of M_1dG was negative (−24.8 kJ mol^{-1}), indicating the favorability of the reaction at 1 M hydroxide and M_1dG. The free energy change of the reaction was largely dominated by the drop in enthalpy (−21.9 kJ mol^{-1}) when measured at the temperatures used in this assay, and the contribution of the entropy change was small.

Three independent approaches were used to establish the value of K_{eq}, and similar values were obtained by each. Using the equilibrium constant derived from kinetic studies, the ratios of N^2OPdG$^-$ to M_1dG at different pHs were calculated (Table 4). At pH 11.0, the equilibrium lies toward the ring-opened form (N^2OPdG$^-$/M_1dG is 21.5:1), corresponding to nearly 95% conversion of N^2OPdG$^-$. However, at neutrality, the equilibrium shifts dramatically toward M_1dG (N^2OPdG$^-$/M_1dG is 1:465) so that less than 1% of the adduct is in the ring-opened form.

The conversion of M_1dG to N^2OPdG$^-$ was demonstrated to be first-order with respect to M_1dG and hydroxide and second-order overall. The fact that the plateau of the fluorescence change decreased as a function of increasing hydroxide concentration indicated that changes in hydroxide concentration influence the position of the equilibrium. Thus, hydroxide must be a reactant rather than a catalyst in the conversion. The fact that the plot of k_{obs} versus hydroxide concentration was linear with a nonzero intercept supported this conclusion. As described above, the rate of ring-closure dominated the equilibrium only when hydroxide concentration was low. On the basis of these findings, we propose the mechanism in Figure 10. Direct attack on C8 of M_1dG by hydroxide leads to the transient carbinolamine carbanion which then ring-opens via elimination by C8−N bond breakage. The formal negative charge is delocalized throughout the structure as a number of resonance and tauto-

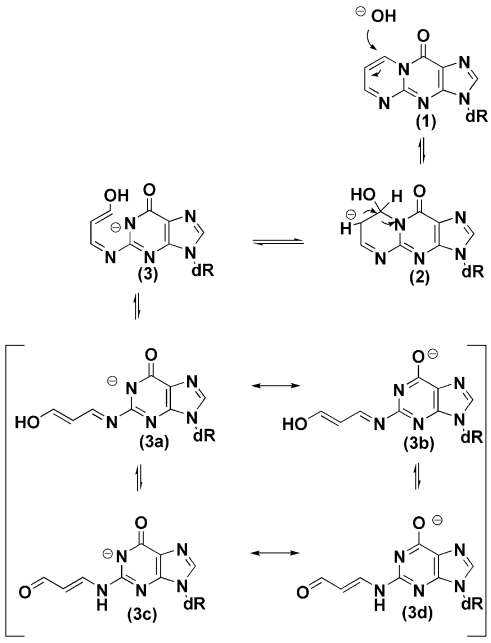

Figure 10. Proposed mechanism for M_1dG ring-opening. Hydroxide adds at C8 of M_1dG **(1)** to give a carbinolamine carbanion **(2)** that opens at the C8−N bond to give an N1 anion **(3)**. This anion is delocalized to O^6 in the series of tautomers and resonance forms shown for the ring-opened anion **(3a−d)**.

meric forms can be drawn for the ring-opened anion. Experiments to be reported separately indicate that N^2OPdG has a pK_a below 7 and will dissociate under the basic conditions used for ring-opening.[27] The reverse reaction depicted in Figure 10 involves ring-closure of the anion followed by elimination of hydroxide to form M_1dG. Protonation of N^2OPdG$^-$ accelerates the rate of ring-closure which proceeds by a different mechanism.[27]

The analyses described above for the nucleoside ring-opening reaction were also completed for oligonucleotides containing M_1dG. Table 3 shows that the forward rate constants for oligonucleotide adduct ring-opening are of comparable magnitude, regardless of sequence context. The forward rate constants are approximately 10-fold lower than that of the nucleoside with an average rate of 0.37 M^{-1} s^{-1}.

The thermodynamics observed for the oligonucleotides were different than those observed for M_1dG. The change in enthalpy was negative and larger in three of the four sequences tested than that observed for M_1dG. However, unlike the nucleoside, the entropic contribution to the reaction was negative for all oligonucleotides tested. Previous reports have demonstrated that regression analysis to obtain values in the *y*-intercept is prone to error.[28] While it is possible that the values observed for enthalpy and entropy may contain some error attributed to van't Hoff analysis, the trends observed for the thermodynamics of ring-opening under basic conditions, with the reaction being dominated by a large negative change in enthalpy and minor contributions seen from changes in entropy, are similar in all the experimental determinations that were made.

At physiological-to-basic pH, the phosphodiester backbone of DNA is ionized and may affect the susceptibility of M_1dG oligonucleotides to nucleophilic attack by hydroxide. Experiments were performed to determine the contribution of the negative charge of oligonucleotide backbones on the observed reduction in forward rate. First, a model nucleotide bearing a 5′-phosphate was used in ring-opening experiments. Studies with M_1dG-5′-phosphate revealed reduced k_{for} values and a greater dependence on the change in enthalpy for the thermodynamics of the reaction with hydroxide when compared with the reaction of the nucleoside adduct (Table 1). Interestingly, the ring-opening reaction for the nucleotide exhibits a doubling of the change in the enthalpy of the nucleoside reaction, displays a negative change in entropy, and in general, resembles the thermodynamic trends observed for oligonucleotides. It is plausible that the negative charges of the phosphodiester backbone have additive effects on the k_{for} observed and is part of the reason for the greater reduction in the forward rate. Despite the differences in the thermodynamics, the difference in the change in the free energy of the nucleoside and nucleotide reactions was small, and K_{eq} for M_1dG-5′-phosphate was large (1.6×10^4 M^{-1}).

The data in Table 3 for different oligonucleotide-sequence contexts show smaller K_{eq} values than that observed for the nucleoside. Also, the data reflect some sequence dependencies for the observed equilibrium constant under basic conditions. It is of note that the sequence dependence observed in these experiments appears to be based upon the identity of the flanking sequences as either pyrimidines or purines, rather than a difference based on species that are charged or uncharged under the basic conditions of the assay. Both guanine and thymine are ionized under the conditions of the assay, whereas adenine and cytidine contain no base-ionizable groups. It is possible that differences in sequence context may produce different three-dimensional environments around the adduct. CD spectroscopy was used to evaluate changes in adduct absorption in the oligonucleotides used in the kinetic assays (Supporting Information 3). Although some differences were observed in the CD of the oligonucleotides, no changes in absorbance could be related to the kinetic and thermodynamic trends described above.

In light of work by Mao et al., it is interesting to note the remarkable contrast in the ring-opening kinetics of M_1dG in a nucleoside or in a single-stranded oligonucleotide compared with ring-opening in duplex DNA.[22] Whereas the equilibrium between M_1dG and N^2OPdG$^-$ is a hydroxide-dependent process favoring M_1dG at neutral pH in the single-stranded oligonucleotide, it is a facile and quantitative conversion to N^2OPdG in the DNA duplex. The fact that ring-opening occurs readily at neutral pH when M_1dG is placed opposite dC indicates the microenvironment of the DNA duplex shifts the equilibrium to the formation of N^2OPdG. More striking is the sequence dependence for ring-opening, where to date only dC in the opposite strand has been shown to shift the equilibrium to the ring-opened form. Work by Stone and colleagues suggests that N^2OPdG projects into the minor groove of duplex DNA and causes minimal distortion in the DNA helix.[21] Efforts to determine the kinetics of ring-opening in the duplex by absorbance or fluorescence spectroscopy were unsuccessful because the absorbance and emission signals were quenched upon duplex annealing. According to NMR experiments, quantitative

(27) Riggins, J. N.; Pratt, D. A.; Voehler, M.; Daniels, J. S.; Marnett, L. J. Kinetics and mechanism of the general acid-catalyzed ring closure of the malondialdehyde−DNA adduct, N^2-(3-oxo-1-propenyl)deoxyguanosine (N^2OPdG$^-$) to 3-(2′-deoxy-β-D-*erythro*-pentofuranosyl)pyrimido[1,2α]-purin-10(3H)-one (M_1dG). *J. Am. Chem. Soc.* **2004**. Submitted for publication.

(28) Exner, O. *J. Phys. Org. Chem.* **1997**, *10*, 797−813.

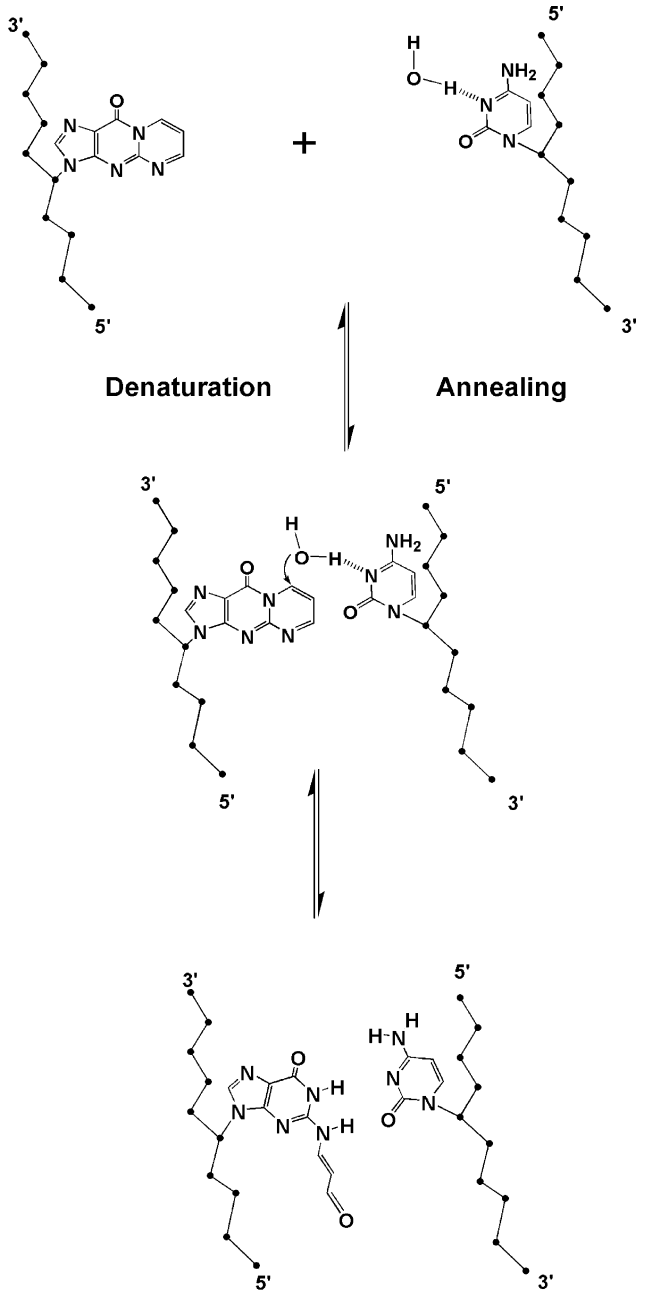

Figure 11. A proposed model for M_1dG ring-opening in duplex DNA. Upon annealing with its complement, M_1dG in an oligonucleotide is juxtaposed a hydrated cytosine, which adds hydroxide to M_1dG. The oxopropenyl group of N^2OPdG is protonated in duplex DNA but prevented from recycling by projection into the minor groove.

ring-opening occurs within 5 min of duplex annealing. On the basis of the ring-opening data presented here and the model proposed in Figure 10, we hypothesize the ring-opening reaction in oligonucleotides is driven by duplex annealing (Figure 11). The annealing process brings the complementary cytosine into close proximity to the M_1dG of the complementary strand, and the activation of water by N3 of cytosine facilitates its addition to the adjacent M_1G base. Once ring-opening has occurred, the side chain of N^2OPdG can move into its position in the minor groove, allowing annealing to be completed. The driving force for the reaction then is the formation of the duplex. Once duplex hydrogen bonds have formed, N^2OPdG is "locked" into the ring-opened form. The presence of a hydrated cytosine at the N3 position opposite M_1dG is responsible for the marked increase in the rate of the ring-opening reaction, and duplex formation is responsible for shifting the position of the equilibrium, by preventing ring-closure.

Experimental Section

Materials. All materials were obtained from commercial sources unless otherwise noted. M_1dG and M_1dG-5′-phosphate were synthesized as previously described.[29] M_1dG containing oligonucleotides were synthesized as described and purified by polyacrylamide gel electrophoresis.[29] M_1dG content was verified by MALDI-MS. The sequences used were: **AXA8mer**: 5′-GGAXACCG-3′, **CXC8mer**: 5′-GGCXCCCG-3′, **GXG8mer**: 5′-GGGXGCCG-3′, **TXT8mer**: 5′-GGTXTCCG-3′, where X is M_1dG. Reagents were prepared in buffer (0.01 M sodium phosphate, pH 7.0) and equilibrated at room temperature before use.

Ring-Opening Assay. Ring-opening determined by ^{1}H NMR was completed by combining M_1dG and sodium phosphate buffer, pH 11.2, to final concentrations of 1×10^{-5} M and 0.25 M, respectively. NMR experiments were performed on a Bruker 400 MHz instrument. Data were processed using XWIN NMR. The mixture was allowed to equilibrate at room temperature for 1 h and then frozen and dried under vacuum. The dried solid was then redissolved in D_2O, and ^{1}H NMR was completed using a water presaturation pulse program.

Ring-opening was studied using either fluorescence or UV absorption. Steady-state fluorescence experiments were all conducted on an L-formatted SPEX 1681 Fluorolog spectrofluorometer at various excitation and emission wavelengths. In fluorescence experiments, slit widths were set to 8 mm and the reaction was carried out in a final volume of 1×10^{-4} L (path length 1 cm). Excitation and emission for M_1dG disappearance were monitored at 363 and 511 nm, respectively. M_1dG quantum yield was measured by comparison with quinine sulfate as described.[30] UV spectroscopy was performed on an HP 845X UV spectrometer. Reaction mixtures were equilibrated to the desired temperature in the spectrophotomer cuvette holder, and the reaction was initiated by the addition of concentrated phosphate at various pH values as described in the figure legends. Changes in fluorescence or UV absorption were monitored over time until the ring-opening reaction reached equilibrium. The resultant plots from triplicate experiments were fit to either a one-phase exponential decrease (absorbance data) or a one-phase exponential decrease (fluorescence data) functions ($r^2 > 0.95$) using GraphPad Prism to obtain k_{obs} values. Error was calculated as described.[31]

Acknowledgment. This research was supported by grants from the National Institutes of Health (CA87819 and ES00267) J.N.R. was supported by a training grant (ES07028). We are grateful to D. A. Pratt and N. A. Porter for helpful discussions and to R. N. Armstrong for the use of a fluorescence spectrometer.

Supporting Information Available: Tables of k_{obs} for ring-opening in oligonucleotides and figures demonstrating disappearance of N^2OPdG$^-$ at pH 14 and CD spectra of single-stranded oligonucleotides containing M_1dG. This material is available free of charge via the Internet at http://pubs.acs.org

JA040009R

(29) Schnetz-Boutaud, N. C.; Mao, H.; Stone, M. P.; Marnett, L. J. *Chem. Res. Toxicol.* **2000**, *13*, 90−95.
(30) Guilbault, G. G. *Practical Fluorescence*, 2nd ed.; Marcel Dekker: New York, 1990.
(31) Fersht, A. *Structure and Mechanism in Protein Science: A Guide to Enzyme Catalysis and Protein Folding*; W. H. Freeman and Company: New York, 1999.